(19) Europäisches Patentamt
European Patent Office
Office européen des brevets

(11) Publication number : **0 588 536 A2**

(12) **EUROPEAN PATENT APPLICATION**

(21) Application number : **93306951.0**

(51) Int. Cl.[5] : **H01M 4/86,** H01M 8/12

(22) Date of filing : **02.09.93**

(30) Priority : **03.09.92 US 940031**

(43) Date of publication of application :
23.03.94 Bulletin 94/12

(84) Designated Contracting States :
AT BE CH DE DK ES FR GB GR IE IT LI LU MC NL PT SE

(71) Applicant : **CERAMATEC INC.**
2425 South 900 West
Salt Lake City, Utah 84119 (US)

(72) Inventor : **Khandkar, Ashok C.**
1921 Nevada Street
Salt Lake City, Utah 84108 (US)

(74) Representative : **Rees, David Christopher et al**
Kilburn & Strode 30 John Street
London WC1N 2DD (GB)

(54) **Creep resistant metal-coated LiFeO2 anodes for molten carbonate and solid oxide fuel cells.**

(57) A porous, creep-resistant, metal-coated, $LiFeO_2$ ceramic electrode for fuel cells. The electrode comprises an ion conducting electrolyte, a layer of unsintered $LiFeO_2$ adjacent the electrolyte and a metal powder in contact with the $LiFe_2$. The metal powder and $LiFeO_2$ are sintered to form a porous electrode.

EP 0 588 536 A2

This invention relates to anodes for molten carbonate fuel cells.

The use of porous nickel sintered plaques as electrodes in molten carbonate fuel cells has been widespread. In general, these electrodes are high performance electrodes, but suffer from two pivotal problems. The first is the high cost of nickel and, secondly, these electrodes continue to sinter with time resulting in a loss of surface area and creep. This in turn results in altered dimensions, altered pore size distribution in the plaque and a concomitant loss of performance over the 50,000 hour required life of an operating cell.

At the anode, hydrogen in the fuel gas reacts with carbonate ions from the electrolyte to form water and carbon dioxide:

$$H_2 + CO_3^{=} = H_2O + CO_2 + 2e^-$$

At the cathode, oxygen and carbon dioxide react to form carbonate via the overall reaction:

$$\frac{1}{2}O_2 + CO_2 + 2e^- = CO_3$$

State-of-the-art molten carbonate fuel cell anodes are porous plaques prepared by sintering a physical mixture of metallic nickel and a variety of stabilising additives in a reducing atmosphere at about 1000°C. The anode provides reaction sites for electrochemical oxidation of hydrogen in the fuel which is enhanced by increased surface area, good electronic conductivity and sufficient wetting by the carbonate electrolyte. Additional functions of the anode include: reservoir for carbonate storage required to replenish that being lost from the cell package; catalyst for the reforming and water gas shift reaction of the fuel; and a bubble pressure barrier to prevent intermixing of fuel and oxidant if flaws develop in the electrolyte matrix. For all these functions, the pore structure and the wetting characteristics of the anode are important, and since the fuel cell is required to endure 40,000 hours of operation, the stability of these properties must be assured.

Current Ni + 2% to 10% Cr anodes have porosities of 60% to 70% and a mean pore size of 3 to 6 μm. As described earlier, the added chromium is converted during cell operation to $LiCrO_2$ which consumes carbonate and causes morphological changes in the electrode. These morphological changes of the anode cause shifts in the carbonate inventory of both the electrolyte matrix and the cathode which results in cell performance changes. In addition, this restructuring of the porous anode facilitates unwanted creep of the anode due to the applied holding forces used to maintain good cell contact and adequate gas sealing around the cell parameter.

Metal-coated ceramic anodes for molten carbonate fuel cells have shown superior creep resistance and therefore have great potential for long life, stable, economical anodes. A major drawback with the choice of the metal/ceramic substrate compositions is the wetting problem, leaving a weak anode.

An electroless metal plating process as described in US Patents 4,361,631; 4,404,267 and 4,423,122 was found to result in non-uniform and incomplete metal coverage, especially on $LiAlO_2$ substrates. Anodes fabricated from metal coated powders were found to have inadequate strength.

The main problems related to the development of metal coated ceramic anodes were shown to be related to dewetting of the metal at elevated temperatures of anode fabrication. Metal coated $SrTiO_3$ powders were made into anodes by a process identical to that in the above prior art patents. Microstructural examination revealed that the grains of the ceramic had fused together, with the metal having dewetted from the surface of the ceramic.

Another problem related to the Cr-stabilised Ni anode is that during cell operation, the Cr undergoes corrosion to form $LiCrO_2$ through reaction with the Li_2CO_3-K_2CO_3 (62-38 mol ratio) electrolyte.

It is an object of the present invention to overcome these drawbacks.

According to one aspect of the invention, there is provided a creep-resistant electrolyte/electrode structure for a high-temperature fuel cell comprising: an ion conducting electrolyte; a layer of unsintered particulate $LiFeO_2$ adjacent the electrolyte; and a conductive metal powder in contact with the particulate $LiFeO_2$, the metal powder and particulate $LiFeO_2$ being sinterable to a porous, electro-conductive creep-resistant electrode in electro-conductive contact with the electrolyte.

Thus, a creep-resistant, metal-coated $LiFeO_2$, ceramic electrode for molten carbonate fuel cells (MCFC) has been developed.

A $LiFeO_2$ powder substrate, when coated with metal, especially nickel and nickel alloys, and sintered to form a porous anode, forms a creep resistant anode which does not exhibit significant dewetting problems. The metal coating adheres well to the ceramic powder and forms a continuous conduction path. The average creep of such anodes is -2.5-3%, which is significantly better than state-of-the-art Ni(Cr) anodes. Conceptually, by using a significant volume of a low-cost ceramic substrate, problems related to sintering and morphological changes due to creep can be greatly reduced. Moreover, the absence of Cr as a stabiliser is expected to reduce corrosion/lithiation, thus allowing stable long-term performance. Cu/Ni-coated (50:50 mol ratio, 50 w/o metal loading) $LiFeO_2$ anodes were optimised to meet MCFC anode specifications.

Creep testing of the metal coated ceramic anodes was conducted. From the creep result it was determined that the predominant creep mechanism is due to particle rearrangement. The anode porosity and mean pore

size had significant effect on the creep of the anode. Lower porosity and pore size consistent with performance criteria are desired to reduce creep. Lower metal loading with uniformity of coverage will result in lower creep behaviour of the anode. Of the substrate evaluated, $LiFeO_2$ in general exhibited lower creep which was attributed to superior metal adhesion. Such Ni metal coated $LiFeO_2$ anodes can be also used as anodes for low temperature solid oxide fuel cells (SOFCs).

A critical requirement of such anodes is that the metal (Ni or Ni-Cu alloys) form a continuous film over the ceramic powder substrates thus allowing continuous electronic conduction paths. Figure 1 shows schematically the ideal metal coated ceramic anode morphology. The thin metal layer on the ceramic particles is expected to show substantially increased creep resistance. Further advantages of this approach are that anode morphology can be better controlled by controlling the size of the ceramic (substrate) powder and the metal coating thickness. In addition, substantial cost reductions are also expected by using reduced amounts of metal and low cost ceramic substrates.

Preferably, the unsintered particulate $LiFeO_2$ has a particle size of between 5 μm and 8 μm. The metal may be nickel or a nickel alloy, preferably a Ni/Cu alloy. Preferably, the Ni/Cu alloy is 40 mol% to 60 mol% Ni. Satiable anode materials were prepared by coating by electroless deposition techniques 50 Ni/50 Cu on a conductive ceramic ($LiFeO_2$) substrate.

Preferably, the metal loading is from 30% to 60%, and is preferably less than 40%. Preferably, the metal powder is applied to the particulate $LiFe0_2$ by electrode deposition or chemical vapour deposition. In a preferred form, the sintered metal coated $LiFe0_2$ electrode has a thickness of from 0.5 μm to 1 μm.

The fuel may be a molten carbonate fuel cell and the electrolyte is a carbonate ion conducting electrolyte. Alternatively, the cell may be a solid oxide fuel cell and the electrolyte is an oxygen ion conducting metal oxide electrolyte.

According to a second aspect of the invention, there is provided a creep-resistant electrode composition of an MCFC comprising an electro-conductive sintered metal coated $LiFeO_2$ particulate structure having a porosity of 30% to 50%.

The invention may be carried into practice in various ways and some embodiments will now be described with reference to the accompanying drawings, in which:-

Figure 1 is a schematic representation of metal coated ceramic particles;

Figures 2 and 3 are photomicrographs of sintered Cu/Ni on $LiFeO_2$;

Figures 4 and 5 are graphs which show the creep behaviour of metal;

Figure 6 is a graph which illustrates the effect of temperature on the shrinkage of $LiFeO_2$ anodes;

Figure 7 is a graph which illustrates the effect of consolidation pressure on the porosity of $LiFeO_2$ anodes;

Figures 8(A) and 8(B) are photomicrographs of metal coated anodes;

Figure 9 is a diagram of a cell package test stand; and

Figure 10 is a graph showing the creep characteristics of $LiFeO_2$ material.

A large batch of $LiFeO_2$ was synthesised. The powder was determined to be phase pure using XRD, and the particle size distribution and BET surface area were characterised. The powder was milled to get a mean particle size centred around 15 μm. The metal wetting characteristics were found to be favourable as compared to $LiAlo_2$. An electroless Ni and Cu plating process was developed and the optimal conditions were determined. The metal coating appeared to be uniform as determined by SEM/EDXS. In a separate study, the phase stability of $LiFeO_2$ in a molten carbonate melt was determined.

Anodes were made from $LiFeO_2$ particles with Ni, Cu or Ni/Cu alloys. The sintered anodes exhibited good mechanical properties. SEM examination of the microstructure revealed good coating of the particles with well formed necks thus confirming the observed strength of sintered anodes. Typical microstructures are shown in Figures 2 and 3. After several fabrication trials, it was determined that moderate pressure during sintering improved the strength of the porous anode plaques. The porosity of the sintered plaques were varied by varying the compaction pressure.

There was much scatter to the results. Of all the tests, the Ni-Cr electrodes showed the least creep. The creep ranged from a low 0.65% to a high of 6.18% and were the most consistent. The $LiAlo_2$ electrodes creep values ranged from a low of 0.96% to a high of 20.23%. The $LiFeO_2$ electrodes had the most scatter and creep ranged from a low of 1.46% to a high of 33.93%. Summarising the results for metal coated $LiFeO_2$ powder, with approximately 37% metal loading and 45% porosity and average of 4 samples indicate a creep of 3.6% at 650°C; 100 psi (689 kPa). This is an improvement over state of the art materials.

Table I

$LiFeO_2$ at 650°C and 100 psi (689 kPa)						
Metal						
Test No.	Loading					
2.3.1b-10	50.49	9.0	27.63	7.11	LF-18	6
2.3.1b-05	37.0	6.0	48.7	4.31	LF-10	3
2.3.1b-05	37.0	6.0	48.42	1.45	LF-10	2
2.3.1b-06	37.0	6.0	44.10	2.55	LF-10	1
2.3.1b-06	46.5	6.0	43.8	6.31	LF-9	1
2.3.1b-11	43.33	N/A	40.97	32.12	LF-19	2
2.3.1b-11	66.0	N/A	43.07	32.20	LF-16	5

The metal wetting characteristics of $LiFeO_2$ anodes are more favourable. Thus, a better bond is to be expected between the metal and the ceramic, thereby reducing the amount of primary creep. Figures 4 and 5 show the general trends in the creep behaviour of metalcoated $LiFeO_2$ anodes. Creep is relatively insensitive to both metal loading and anode porosity, indicating that once particle rearrangement occurs secondary creep mechanisms dominate the creep behaviour. Creep characteristics are shown for Test ≠ -5. The data show that the magnitude of the primary creep is less than ~2%. Further creep is as expected for diffusion driven process. Higher anode creep is exhibited for anodes with higher means pore size and porosity. This is consistent with observations for $LiAlO_2$ anodes. However, the overall creep characteristics are superior for metal coated $LiFeO_2$ and it exhibits the potential for a viable alternative anode material.

Metal-coated $LiFeO_2$ anodes show great potential as a creep resistant anode. Further improvements in both metal adhesion as well as anode morphology are anticipated which could lead to reduced primary creep and thus enhance creep resistance. These anodes generally meet the functions of the molten carbonate fuel cell anode which are:

- Provide reaction sites for electrochemical oxidation the fuel gas
- Act as fuel reforming catalyst
- Serve as reservoir for storage of electrolyte for carbonate management of the cell package
- Act as a bubble pressure barrier when fabricated as a dual porosity structure

To perform these functions, the anode must have:

- High exchange current density
- Good electrocatalytic activity
- Good electrical conductivity
- Low oxidation potential
- Good wetting characteristics to hold carbonate
- High catalytic activity towards fuel reforming reactions
- Appropriate porosity and pore size distribution
- Good mechanical strength
- Sufficient thickness to store the carbonate requirements of life.

TABLE 2 ANODE STRUCTURE TRADE-OFFS

Goal		Desired Structure
Strength and Dimensional Stability	1.	Low porosity
	2.	Small pores
Low Polarisation	1.	Large pores for fuel access
	2.	Large surface small particles
Carbonate Reservoir	1.	Some pores larger than Electrolyte Matrix pores
	2.	Thick layer
	3.	High porosity
	4.	Large population of small pores
Reforming Catalyst	1.	Large surface area

Clearly, the optimum anode structure with respect to a specified electrolyte and cathode structures must be determined on a "case-by-case" basis for each candidate anode type/structure. The metal coated $LiFeO_2$ anode materials possess, generally, the desired characteristics for good anode materials.

$LiFeO_2$ Synthesis

$LiFeO_2$ powder was synthesised using the following procedure: Li_2CO_3 and Fe_3O_4 were mixed in stoichiometric proportions and ball milled for 12-14 hours in ethanol. The mixture was then dried and calcined in a crucible in air at 1200°C for 10 hours. The resulting agglomerated powder was ball milled for 2 hours and recalcined at 1200°C for 10 hours to ensure complete reaction and homogeneity. The synthesised powder was characterised by XRD to confirm the $LiFeO_2$ phase.

Among the two large (~1kg) batches of $LiFeO_2$ synthesised, the first batch was found to be a mixture of alpha-$LiFeO_2$ and alpha-$LiFe_5O_8$; the Li deficient phase, alpha-$LiFeO_5O_8$, results from a loss of lithia during calcination/reactive-sintering cycles during synthesis. The second batch was synthesised in an effort to achieve a single phase of $LiFeO_2$. During the sintering cycles, some Li_2CO_3 was sprinkled over the powder mass, in order to avoid the loss of lithia. The top layer of the powder was discarded and the rest of the powder was milled to break up agglomerates and then characterised by XRD. This powder was characterised to be single phase alpha-$LiFeO_2$.

Sintering Trials on Cu/Ni Coated $LiFeO_2$

The past efforts were centred principally on pressureless sintering of metal coated ceramic powders and prepressing at various pressures followed by pressureless sintering. SEM examination of the sintered anodes showed that while the particles were of the approximate size range compatible with achieving the desired anode specifications, the packing of the particles was not optimum. A "honeycomb" type structure was formed due to interparticle necking of the metal deposits. This resulted in large agglomerates with large open pores.

Efforts were centred around adding binders to the metal coated ceramic powders and prepressing them to different pressures. In addition to these trails, two more trials were conducted using a magnetic field to align the particles in the graphite die in order to obtain better and more uniform particle packing. The parameters are tabulated in Table 3.

These samples were analysed to determine if there was any trend or relationship between fabrication con-

ditions and the resulting density and mean pore size (MPS). A porosity of 50 to 60% with a mean pore size of 35 μm are desired.

Variations in the thickness of the plaques of 5-8 mils (127-203 μm) were observed. Generally, the samples were thinnest at the centre and thickest at the edges. The variations in plaque thickness may be a source of density gradients within the samples.

Table 3

Sintering Variations for Anode Fabrication Trials		
Sample Code	Sample ID	Sintering Conditions
31	5NF140	0.2 w/o PVB in acetone; 250 psi (consolidation pressure; 126 g.load; gravity sintering.
32	5NF140	($LiFeO_2$ with 0.5 w/o Elvacite) 250 psi (1.7 MPa) consolidation pressure; 126 g.load; "pressureless" sintering.
33	5NF142	vibratory packing in mag. field; 100 psi (0.69 MPa) consolidation pressure; hot press T=925°C, 1000 psi.
34	5NF142	vibratory packing in mag. field; 100 psi (0.69 MPa) consolidation pressure; 126 g.load; pressureless sintering (T=925°C).

A total of 11 different anode specimens were fabricated and the processing conditions are listed in Table 4.

Fabrication Characteristics of Metal-coated $LiFeO_2$ Powders

Three anode fabrication trials were conducted to determine the shrinkage and porosity characteristics of metal-coated $LiFeO_2$ porous compacts. The shrinkage of the $LiFeO_2$ anodes is considerable as compared to the $LiAlO_2$ anodes. As shown in Figure 6, the mean shrinkage upon firing at 925°C for 1 hr is 36% for a consolidation pressure of about 150 psi (1.0 MPa). The porosity of these anodes varies from approximately 48 to 54%. For anodes made at different consolidation pressures and fired at 1100°C for 1 hr, the shrinkage varies from about 32% for a consolidation pressure of about 440 psi (3.0MPa) to a high of about 38% at 6.6 Kpsi (45.5MPa). The porosity variation, shown in Figure 7, is as expected with the highest porosity being exhibited by the anode fabricated at the lowest consolidation pressure.

Fabrication of Metal-coated $LiFeO_2$ Tape Cast Anodes

Several anodes were fabricated by tape casting meal coated $LiFeO_2$ powder. The resultant tapes were thin and very fragile. Four tapes were pressed together at 10,000 psi (68.9MPa). Several anodes 1" (2.5cm) in diameter were punched from the plaque. The geometric densities (i.e sample weight/sample volume) of the anodes were between 3.45 and 3.89 g/cm^3. A medium pore size of 1.24 and a porosity of 46.4% was determined by the porosimetry of one of the anodes. The skeletal density obtained was 8.18 g/cm^3 which may indicate that the powder used was composed primarily of Cu and Ni.

For the purpose of conducting the in-cell tests, it was necessary to fabricate the larger 4" x 4" (10cm x 10cm) anodes for in-cell testing and evaluation. To this end, a large batch of $LiFeO_2$ powder was synthesised and metal coated. Metal-coated $LiAlO_2$ powder was used to cast 8" (20cm) wide tape. Three large green $LiAlO_2$ tape blanks were cut and tested in-cell.

Table 4

Fabrication of Metal Coated $LiFeO_2$ Anodes

Sample No	Processing Condition
4-1	10 μm, $LiFeO_2$, 250 psi(1.7MPa) Consolidation pressure, 126.g.dead load, T=920°C;0.5w/o binder
4-2	same as above but with ~0.7w/o binder
4-3	10μm, $LiFeO_2$, 100 psi(0.69MPa) consolidation pressure, 126g.dead load, T=920°C
4-4	same as 4-3 but with 250 psi(1.7MPa) consolidation pressure
4-5	10 μm, vibratory milled $LiFeO_2$.
4-6	10 μm, ball milled $LiFeO_2$.
4-7	10 μm, ball milled $LiFeO_2$, coated powder crushed lightly in a mortar before sintering to break up necks between particles.
4-8	5 μm, ball milled $LiFeO_2$.
4-9	1 μm, vibratory milled $LiFeO_2$.
4-10	sub-1 μm, vibratory milled $LiFeO_2$.
4-11	1 μm, ball milled $LiFeO_2$ Samples

4-5 to 4-11 were consolidated at 250 psi (1.7MPa) and sintered at 920°C. All of the above samples were sintered in a 90% argon-10% hydrogen atmosphere.

In order o spain the region of possible temperature and compressive forces that a porous anode could encounter in an operating fuel cell, two temperatures (650°C and 700°C) and three holding forces (25, 50 and 100 psi (0.17, 0.34 and 0.69 MPa) were used in earlier tests.

All of the tests which were completed are listed in Table 5. Porosity was used to determine the volume percent porosity, mean pore size, and pore size distribution for each of the anode plaques tested. Initially, the target pore size was 1-3 μm. The mean pore size of plaques tested initially were typically between 7-15 μm. Mean pore sizes of plaques were reduced in further experimentation and were mostly in the range of 4-10 μm. The state-of-the-art nickel-10% chrome anodes are about 65 vol.% porosity and an average pore size of 4-6 μm. The majority of the metal coated $LiFeO_2$ ceramic anodes had 45 to 55 vol% porosity. In general, the metal coated anodes tested had larger pores and a smaller volume percent porosity than the state of the art nickel-chrome anodes.

Chemical analysis was performed to determine the metal-to-ceramic ratio of the anodes materials. The anodes tested were coated with pure nickel or a nickel-copper alloy. The nickel-copper coatings were generally

Table

Batch No.	Test No.	Start	End Date	Rig No.	Test Condi-tioning	Plaque No.	Material	Powder	Load %	%Ni	%Cu	PTS	Poro-sity	% Creep
8	CACT-1	10/29/86	11/05/86	3	650 C. 100PSI	SNP 138-B	$LiFeO_2$	SNP 130-B	50.00	25.00	25.00	18.70	56.80	26.85
5	2.3.1b-05	07/16/87	07/23/87	1	650 C. 100 PSI	XXXX V-1	$LiFeO_2$	LF-18	37.00	18.50	18.50	6.00	67.60	7.63
5	2.3.1b-05	07/16/87	07/23/87	1	650 C. 100 PSI	XXXX V-2	$LiFeO_2$	LF-18	37.00	18.50	18.50	6.00	56.70	2.26
5	2.3.1b-05	07/16/87	07/23/87	1	650 C. 100 PSI	XXXX V-4	$LiFeO_2$	LF-18	37.00	18.50	18.50	6.00	63.90	8.82
5	2.3.1b-05	07/16/87	07/23/87	2	670 C. 100 PSI	XXXI-3	$LiFeO_2$	LF-7	62.67	31.23	31.23	6.00	67.50	
5	2.3.1b-05	07/16/87	07/23/87	2	650 C. 100 PSI	XXXI-4	$LiFeO_2$	LF-7	62.67	31.23	31.23	6.00	53.60	7.63
5	2.3.1b-05	07/16/87	07/23/87	3	650 C. 100 PSI	XXXXI X-1	$LiFeO_2$	LF-10	37.00	18.50	18.50	6.00	63.10	2.62
5	2.3.1b-05	07/16/87	07/23/87	3	650 C. 100 PSI	XXXXI X-2	$LiFeO_2$	LF-10	37.00	18.50	18.50	6.00	63.75	.69
6	2.3.1b-06	07/24/87	08/08/87	2	650 C. 100 PSI	XXXX VIII-2	$LiFeO_2$	LF-10	37.00	18.50	18.50	6.00	44.10	2.55
6	2.3.1b-06	07/26/87	08/08/87	3	650 C. 100 PSI	XXXIII -2	$LiFeO_2$	LF-9	46.50	23.20	23.20	6.00	63.80	
10	2.3.1b-10	11/25/87	12/01/87	1	650 C. 100 PSI	LXXX XVI-1	$LiFeO_2$	LF-18	50.49	33.00	17.49	9.00	26.87	
10	2.3.1b-10	11/25/87	12/01/87	1	650 C. 100 PSI	LXXX XVI-2	$LiFeO_2$	LF-18	50.49	33.00	17.49	9.00	27.37	
10	2.3.1b-10	11/25/87	12/01/87	1	650 C. 100 PSI	LXXX XVI-3	$LiFeO_2$	LF-18	50.49	33.00	17.49	9.00	27.11	
10	2.3.1b-10	11/25/87	12/01/87	2	650 C. 100 PSI	LXXX XVII-1	$LiFeO_2$	LF-18	50.49	33.00	17.49	9.00	29.21	
10	2.3.1b-10	11/25/87	12/01/87	2	650 C. 100 PSI	LXXX XVII-2	$LiFeO_2$	LF-18	50.49	33.00	17.49	9.00	30.12	
10	2.3.1b-10	11/25/87	12/01/87	2	650 C. 100 PSI	LXXX XVII-3	$LiFeO_2$	LF-18	50.49	33.00	17.49	9.00	27.18	
11	2.3.1b-11	03/29/88	04/06/88	1	650 C. 100 PSI	156-2	$LiFeO_2$	LF-19	63.66	21.66	21.66		43.20	
11	2.3.1b-11	03/29/88	04/06/88	1	650 C. 100 PSI	156-3	$LiFeO_2$	LF-19	63.66	21.66	21.66		40.74	
11	2.3.1b-11	03/29/88	04/06/88	2	650 C. 100 PSI	158-2	$LiFeO_2$	LF-16	66.00	33.00	33.00		42.82	
11	2.3.1b-11	03/29/88	04/06/88	2	650 C. 100 PSI	158-3	$LiFeO_2$	LF-16	66.00	33.00	33.00		42.84	
11	2.3.1b-11	03/29/88	04/06/88	3	650 C. 100 PSI	200-1	$LiFeO_2$	LF-16	66.00	33.00	33.00		44.29	
11	2.3.1b-11	03/29/88	04/06/88	3	650 C. 100 PSI	200-2	$LiFeO_2$	LF-16	66.00	33.00	33.00		41.72	
11	2.3.1b-11	03/29/88	04/06/88	3	650 C. 100 PSI	200-3	$LiFeO_2$	LF-16	66.00	33.00	33.00		38.58	

Note: 100psi $\approx$ 0.69MPa

about 50wt% each metal. The amount of metal in the samples or metal loading varied between 10 and 60 wt% (see Table 5).

Scanning electron photomicrographs of polished cross-sections of the anode plaques before testing showed the quality of the materials produced were consistently improved. Photomicrographs showing an excellent microstructure are depicted in Figures 8(A) and 8(B).

IN-CELL TESTING

An in-cell test was made using standard boiler-plate hardware, a sintered $LiFeO_2$ anode, a SOA Ni cathode, stainless steel cathode current collector, and a Ni anode current collector were prepared for assembly. The cell package was assembled and then placed in the bench-scale test stand. A diagram of how the cell package is set up in the test stand is shown in Figure 9.

Three nickel coated $LiAlO_2$ tapes and one nickel coated $LiFeO_2$ tape size large enough to test in bench-scale (94 cm^2) 54% metal loading were sintered and prepared for creep and bench-scale fuel cell tests. A Ni/$LiAlO_2$ tape and the Ni/$LiFeO_2$ tape were sintered in a standard muffle furnace, also purged with cracked ammonia gas. The heating schedule followed was:

4 hours ramped to 850°C
1 hour ramp to 950°C
15 minute hold at 950°C
Cool.

A $LiFeO_2$ electrode which had 54% metal loading, a thickness from 0.0233 inch (0.6 mm), was tested. The cell package was assembled using a state-of-the-art (SOA) nickel cathode and hot-pressure tile. The test was begun using a normal slow ramp heat-up (room temperature to 350°C in 3 hours, from 350°C to 650° in 18 hours). The initial cell performance was poor compared to a SOA cell; it would not hold a stable voltage at 140 mA/cm^2 load, and the resistance was somewhat high at 7.68 m Ω. Increases in the cell holding force which was at 10 psi (69 kPa) initially were applied at 24 (15psi) (103kPa), 143 (20psi) (138kPa), 167 (25 psi) (172kPa), 191 (30 psi) (207 kPa), and 239 (35 psi) (241 kPa) hours. The reason for increasing the holding force was to attempt to improve the contact of the anode to the tile in case the resistance, and poor performance, were due to poor surface contact between the anode and electrolyte. (The poor contact may have been due to the thickness variation of the electrode). A table showing the cell performance mV, IR-free mV, and polarisation mV is shown in Table 6.

TABLE 6

Cell Test CerLiFe-1 Life Data

Hours→	0	24	48	72	144	168	192	216	312	336	360
mA/cm²	Cell millivolts										
0(OCV)	992	988	986	987	991	990	989	994	989	989	987
40	876	877	871	853	811	841	837	847	843	845	843
60	812	823	806	790	737	775	774	779	774	778	784
80	733	770	744	721	653	698	688	708	694	704	703
100	660	707	675	644	547	617	610	625	613	630	619
120	577	645	606	572	455	540	529	548	540	548	555
140	498	576	531	491	363	463	454	475	467	483	483
160		510	462	416	273	387	381	406	396	417	424
180		432	367	330		314	308	326	336	356	351
200									266	284	
220											
240											
resistance	7.68	7.85	8.96	10	10.2	10.7	9.75	9.9	7.96	7.8	7.89

IR free millivolts

mA/cm²												
	40	907	908	907	893	852	884	876	887	875	876	875
	60	858	870	860	850	798	839	833	838	822	825	831
	80	794	833	816	801	735	784	766	787	758	766	766
	100	737	786	765	744	649	724	708	724	693	708	698
	120	669	739	714	692	577	668	646	667	636	642	650
	140	606	686	656	631	506	613	591	614	578	592	593
	160		636	605	576	436	558	537	564	523	542	550
	180		573	528	510		507	484	504	479	496	493
	200									409	424	
	220											
	240											

Polarization millivolts

mA/cm2												
	40	85	80	79	94	139	106	113	107	114	113	112
	60	134	118	126	137	193	151	157	156	167	164	156
	80	198	155	170	186	256	206	223	207	231	223	221
	100	255	203	221	243	342	266	282	270	296	281	289
	120	323	249	272	295	414	322	343	327	353	347	337
	140	386	302	330	356	485	377	399	380	411	397	394
	160		352	381	411	555	432	452	430	466	447	437
	180		415	458	477		483	506	490	510	493	494
	200									580	565	
	220											
	240											

IR FREE mV = mV at load plus resistance in milli-ohms times amps at load setting
i.e. 7.68 milli-ohms times ((100 cm2 x 160mA/cm² = 16000mA)/1000) = 122.88 mV
Polarization voltage equals OCV millivolts minus IR free millivolts

The cell was terminated after 360 hours of cell life, since little improvement was observed after the last cell holding force increase. The terminated anode and current collector were measured and compared to the pre-test anode measurements. Allowing for the thickness of the current collector, which was subtracted from the total measurement since it could not be separated from the anode, the change in anode thickness from pre-test to post-test was 2.6 mils (66μm). This change, based on the pre-test thickness of 19.7 mils (500 μm), corresponds to a 13.2% creep value for the anode.

TABLE 7

Comparison of IR Loss, IR-Free, and Polarisation

Cell Test CerLife-1

Date	Hours	OCV	Load Voltage, mV — mV at 100 mA/cm²	mV at 160 mA/cm²	IR-Loss @ 160 mA	IR-Free @ 160 mA	RES. mΩ	Polarizatio n @ 160 mV/cm²
1988								
4/12	0	992	660	N/A	123	N/A	7.7	N/A
4/13	24	988	707	510	125	635	7.8	353
4/14	48	986	675	462	142	604	8.9	382
4/15	72	987	644	416	160	576	10.0	411
4/18	144	991	547	273	163	436	10.2	555
4/19	168	990	617	387	171	558	10.7	432
4/20	192	989	610	381	155	536	9.7	453
4/21	216	994	625	406	158	564	9.9	430
4/22	240	991	621	394	139	533	8.7	458
4/25	312	989	613	396	127	523	7.96	466
4/26	336	989	630	417	125	542	7.8	447
4/27	360	987	619	424	126	550	7.89	437
Data from a normal SOA fuel cell with Ni+Cr Anode (Cell Test IGT-83-5AC):								
	192	991	847	758	85	843	5.32	148

As can be seen from Table 7, the performance of this cell was inferior to SOA performance. From Table IV it can be seen that the OCV of the cell was acceptable indicating the proper electrochemical potentials each side of the cell (no gas crossover). This was corroborated by measuring the gas crossover during cell life. However, looking at the cell potential at 160 mA/cm² and 192 hours, it can be seen that it is about 377 mV (758-381) lower than a SOA cell whose test results are depicted at the bottom of Table 7 (just the first 360 hours of a 528 hour test are shown for comparison). This 377 mV lower performance is made up from 70 mC higher IR (155-85) and 305 mV higher polarisation loss (453-148). That is, most of the observed lower performance is due to polarisation losses which are most likely due to the active three phase contact on this metal coated $LiFeO_2$ anode not being optimised in this first test. This factor is encouraging since the particle size and the electrode morphology can be developed to match more closely that of a SOA electrode.

The pre-test sample was analysed for Ni, Cu, Fe and Li by atomic absorbtion of a completely dissolved anode solution. The percentages of Fe and Li in the samples were converted to percentages of Fe_2O_3 and Li_2O, which may be combined to represent $LiFeO_2$ or Li_xFeO_2 in case of non-stoichiometry.

Table 8

Chemical Analysis		
Components	Pre-test	Post-test
Cu	40.84	35.63
Ni	25.60	22.32
Li	1.20	1.88
Fe	26.61	20.50
K	--	2.23
CO_2	--	3.40
Li_2O	2.57	3.72
Fe_2O_3	38.04	29.34
K_2CO_3		3.94
Li_2CO_3		0.75
Li_2:Fe_2O_3 (by mole)	0.36	0.68
Cu:Ni (by weight)	1.60	1.60
Metal:Fe_2O_3 (by weight)	1.75	1.98

Results of chemical analysis of pre- and post-test anode are presented in Table 8. The pre-test sample consisted of Cu, Ni and $LiFeO_2$. The Li-to-Fe atom ratio was 0.36, indicating a Li-deficient lithium iron oxide compound which can be represented as $(Li_2O)_xFe_2O_3$ with x = 0.36).

The post-test anode contained Li_2CO_3 and K_2CO_3. To breakdown the total Li to those tied up to $(Li_2O)_xFe_2O_3$ and Li_2OCO_3, CO_2 analysis was performed. Thus, it was assumed that K was converted to K_2CO_3 and CO_2 in excess of that tied up to K was combined with Li to form Li_2CO_3. Excess Li not tied up with CO^2 was then assumed to be tied up with Fe in the form of $(Li_2O)_xFe_2O_3$. The results yield an x = 0.68 post-test. Therefore, the lithiation of the anode took place during cell operation. This is not surprising since one would expect the stoichiometric $Li_2O.Fe_2O_3$ to be stable phase in the presence of electrolyte. In fact, one should start with a stoichiometric $LiFeO_2$ material to prevent lithium consumption from the electrolyte.

The Cu/Ni ratio was similar for both pre- and post-test samples as expected for a sample coated under controlled conditions.

The metal-to-Fe_2O_3 ratio was 1.75 pre-test and 1.98 post-test suggesting slight non-uniformity in metal loading throughout the sample.

The carbonate content of the post-test anode was only 4.69% by weight of 25% filling of the 41% anode porosity. This carbonate content is generally acceptable.

An important observation is the obvious improvement in metal coating coverage on $LiFeO_2$ substrates. This is attributed to the stability of the substrate in the plating bath. It is clear that substrate-bath interactions play an important role, not only in ensuring good unflocculated powder dispersions, but also in ensuring uniformity of surface stabilisation and activation procedures.

Creep Behaviour of Metal-coated $LiFeO_2$ Anodes

In the case of $LiFeO_2$ anodes, the major difference is that the metal wetting characteristics are more favourable. Thus a better bond is to be expected between the metal and the ceramic, reducing the amount of primary creep. Figure 10 shows the general tends in the creep behaviour of metal-coated $LiFeO_2$ anodes. Creep is relatively insensitive to both metal loading and anode porosity, indicative that once particle rearrange-

ment occurs secondary creep mechanism dominates the creep behaviour. Creep characteristics are shown for Test ≠ 2.3.1b-5. The data show that the magnitude of the primary creep is less than ~2%. Further creep is as expected for diffusion driven process. The data for rig 2 for anodes with higher metal loading are inconsistent with the trend and should be disregarded due to a malfunctioning test rig. The effect of anode morphology is greater, with higher anode creep exhibited for anodes with greater mean pore size and porosity. This is consistent with observations of $LiAlO_2$ anodes.

Conclusions

In summary, the following points emerge from the analysis of the microstructure/creep measurements relations.

1. For any metal-coated ceramic anodes, the predominant creep mechanism is due to particle rearrangement. This mechanism will dominate creep behaviour even if the metal wets the ceramic but does not adhere well.
2. The anode porosity must be as low as possible consistent with anode performance criteria such as polarisation phenomena associated with mass transport limitations in such porous electrodes. The mean pore size must also be as low as possible, consistent with performance criteria.
3. Metal coated anodes will exhibit lower creep at lower metal loadings. In fact, the data suggest that completeness of coverage is not the important criterion. Rather, uniformity of metal deposition is more important. It is conceivable that if the metal deposits adhere well, then in a three dimensional porous structure there can be contiguity of metal contacts leading to anode conductivity.
4. The factors affecting metal coating coverage have been mentioned earlier. One consideration is the deposition of metal alloys. In any process which deposits metal sequentially, the driving force for alloy formation will generally exceed the force for wetting (and hence adhesion) on the ceramic. This could also lead to some Kirkendall porosity at the metal/ceramic interface. These factors will weaken the bond and thus lead to poor mechanical properties. Thus, there may be advantage in deposition of alloys on the surface.

Claims

1. A creep-resistant electrolyte/electrode structure for a high-temperature fuel cell comprising: an ion conducting electrolyte; a layer of unsintered particulate $LiFeO_2$ adjacent the electrolyte; and a conductive metal powder in contact with the particulate $LifeO_2$, the metal powder and particulate $LiFe0_2$ being sinterable to a porous, electro-conductive creep-resistant electrode in electro-conductive contact with the electrolyte.

2. A structure as claimed in Claim, characterised in that the unsintered particulate $LiFe0_2$ has a particle size of between 5 μm and 8 μm.

3. A structure as claimed in Claim 1 or Claim 2, characterised in that the metal is nickel or a nickel alloy, preferably a Ni/Cu alloy.

4. A structure as claimed in Claim 3, characterised in that the Ni/Cu alloy is 40 mol% to 60 mol% Ni.

5. A structure as claimed in any preceding Claim, characterised in that the metal loading is from 30% to 60%, and is preferably less than 40%.

6. A structure as claimed in any preceding Claim, characterised in that the metal powder is applied to the particulate $LiFe0_2$ by electrode deposition or chemical vapour deposition.

7. A structure as claimed in any preceding Claim, characterised in that the sintered metal coated $LiFe0_2$ electrode has a thickness of from 0.5 μm to 1 μm.

8. A structure as claimed in any preceding Claim, characterised in that the fuel cell is a molten carbonate fuel cell and the electrolyte is a carbonate ion conducting electrolyte.

9. A structure as claimed in any of Claims 1 to 7, characterised in that the fuel cell is a solid oxide fuel cell and the electrolyte is an oxygen ion conducting metal oxide electrolyte.

10. A creep-resistant electrode composition of an MCFC comprising an electro-conductive sintered metal coated $LiFeO_2$ particulate structure having a porosity of 30% to 50%.

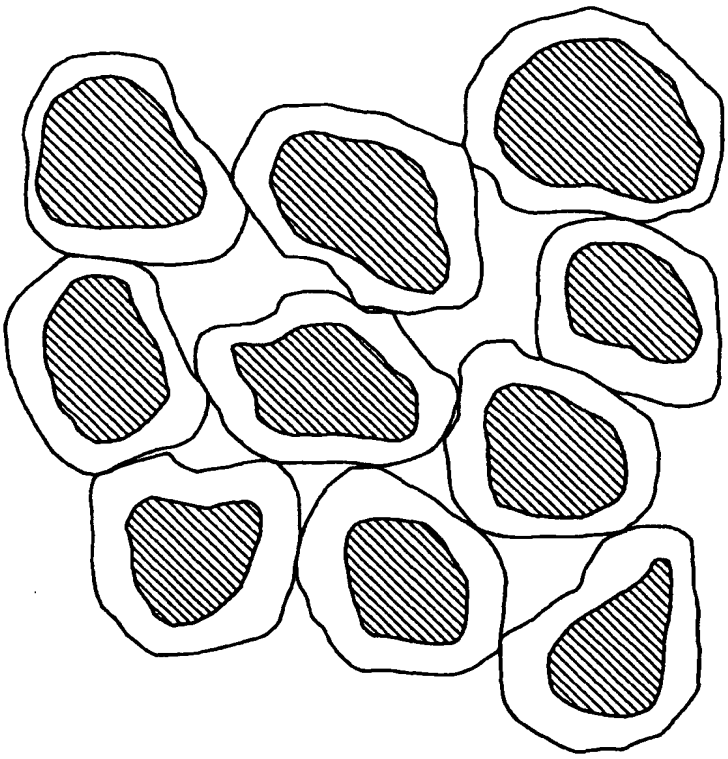

Fig. 1

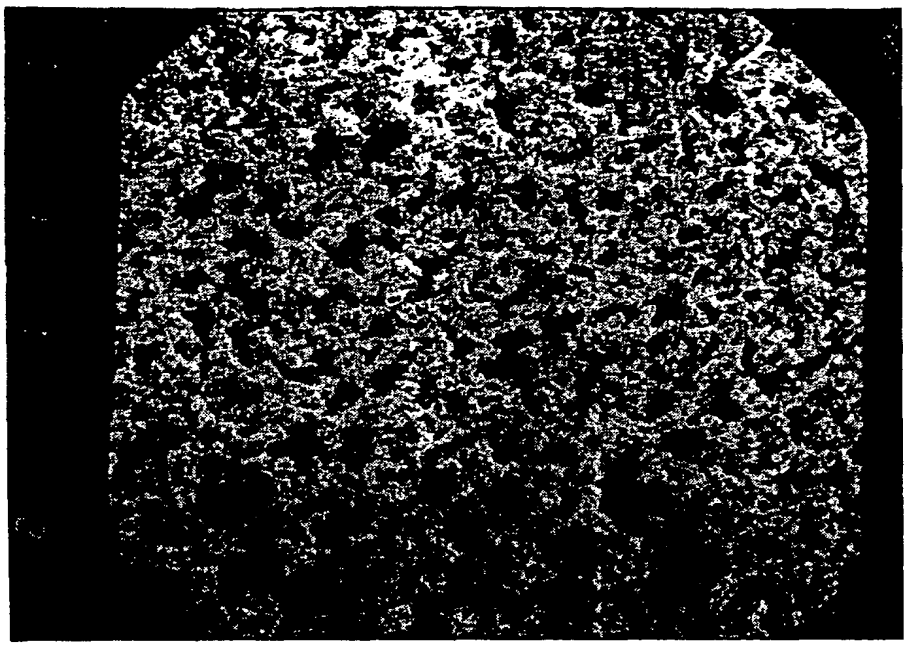

Fig. 2 SINTERED Cu/Ni ON $LiFeO_2$ - 1,00X

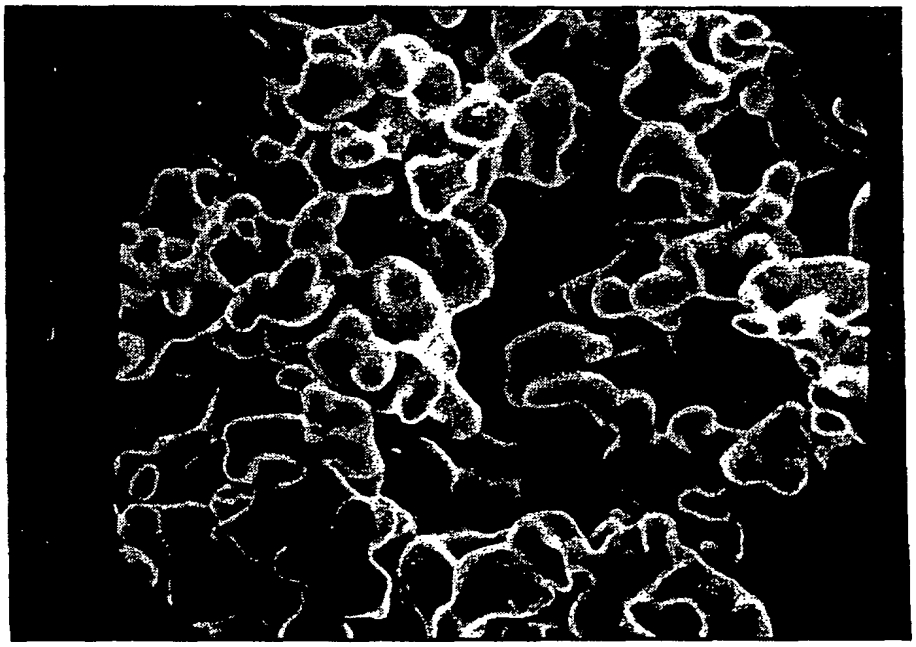

Fig. 3 SINTERED Cu/Ni ON $LiFeO_2$ - 1,000X

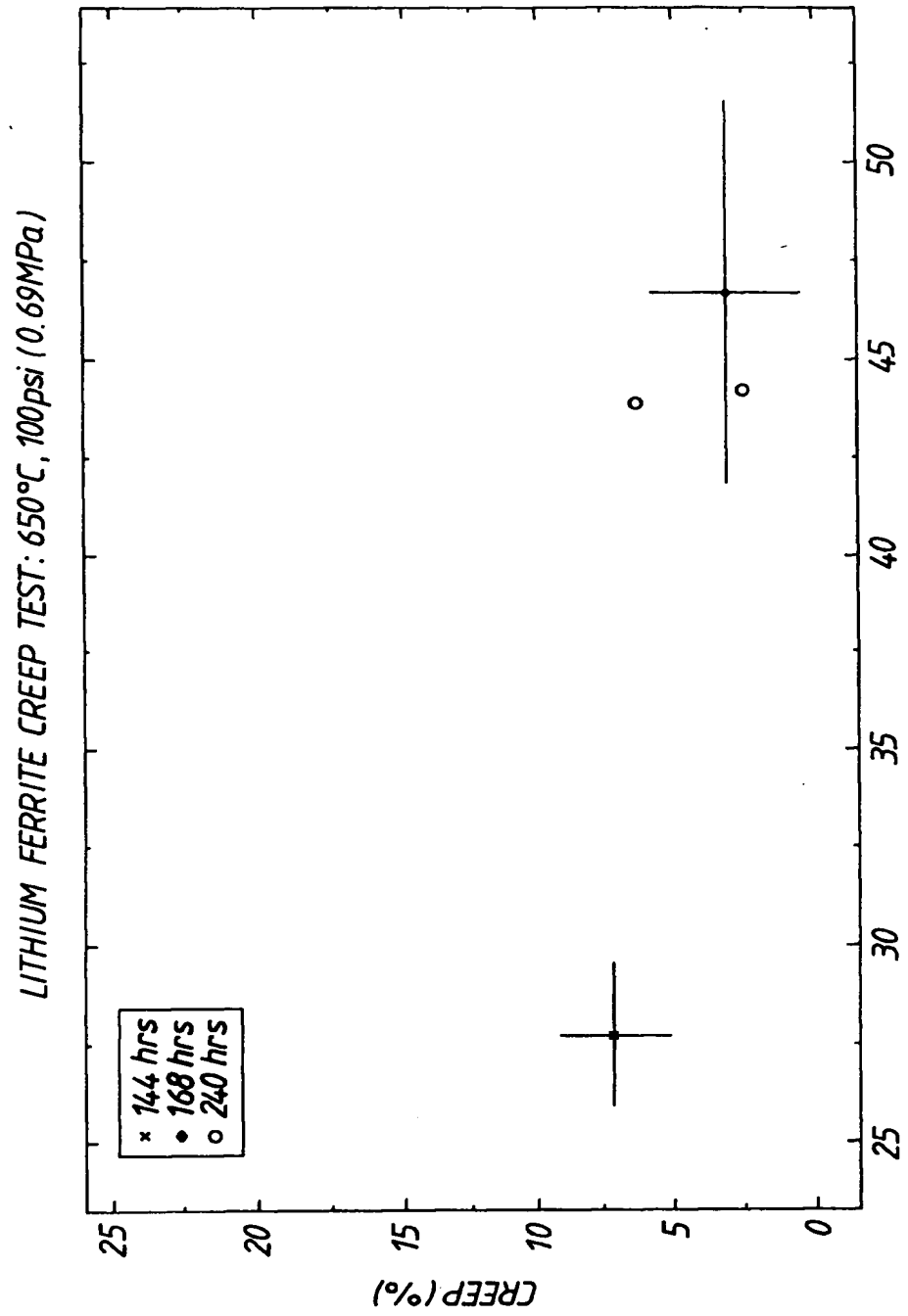

Fig. 4 LITHIUM FERRITE: CREEP AS A FUNCTION OF ANODE POROSITY

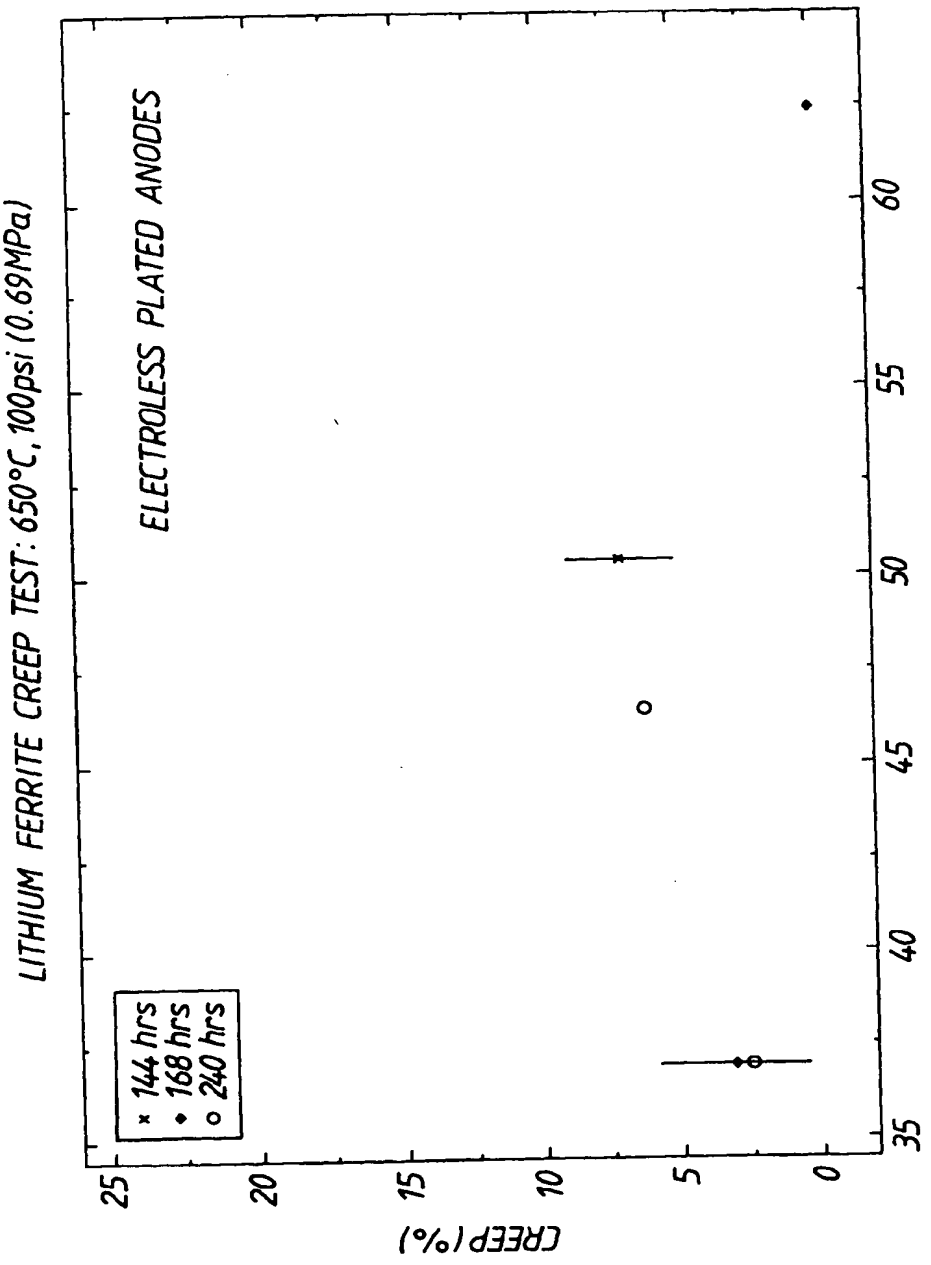

Fig. 5 LITHIUM FERRITE: CREEP AS A FUNCTION OF METAL LOADING

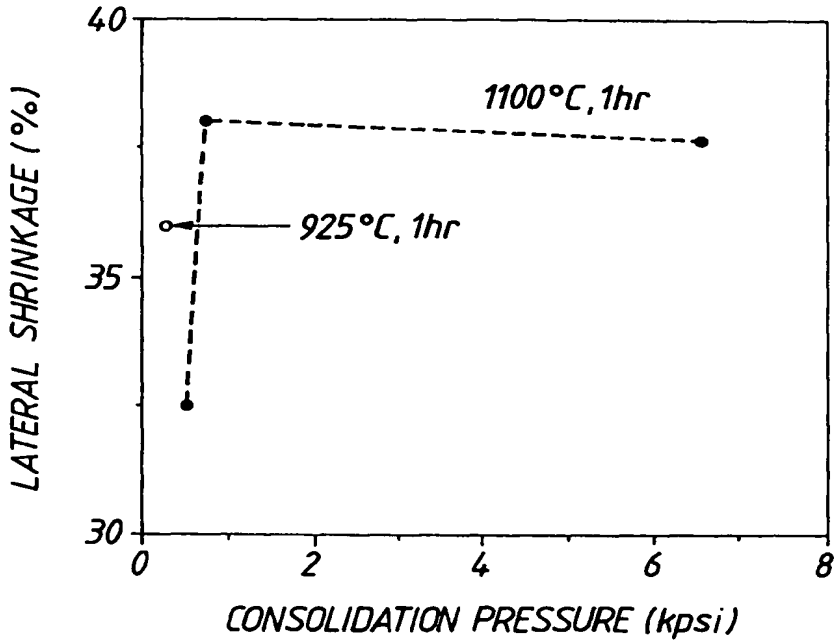

EFFECT OF SINTERING TEMPERATURE ON THE SHRINKAGE OF LIFE O_2 ANODES

Fig. 6

[NOTE – 1 kpsi ≃ 6.89 MPa]

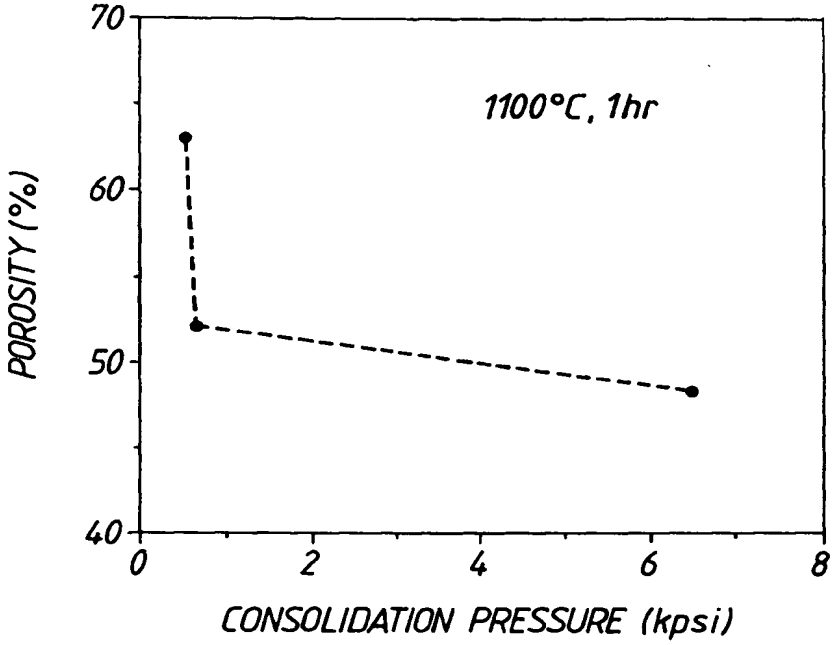

EFFECT OF SINTERING CONSOLIDATION PRESSURE ON THE POROSITY OF LIFE O_2 ANODES

Fig. 7

[NOTE – 1 kpsi ≈ 6.89 MPa]

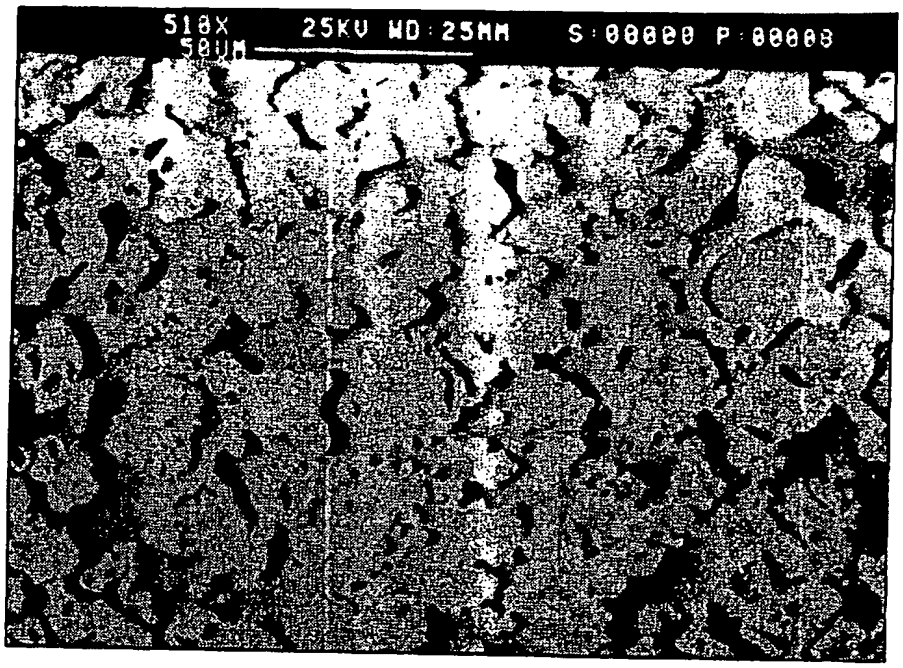

A

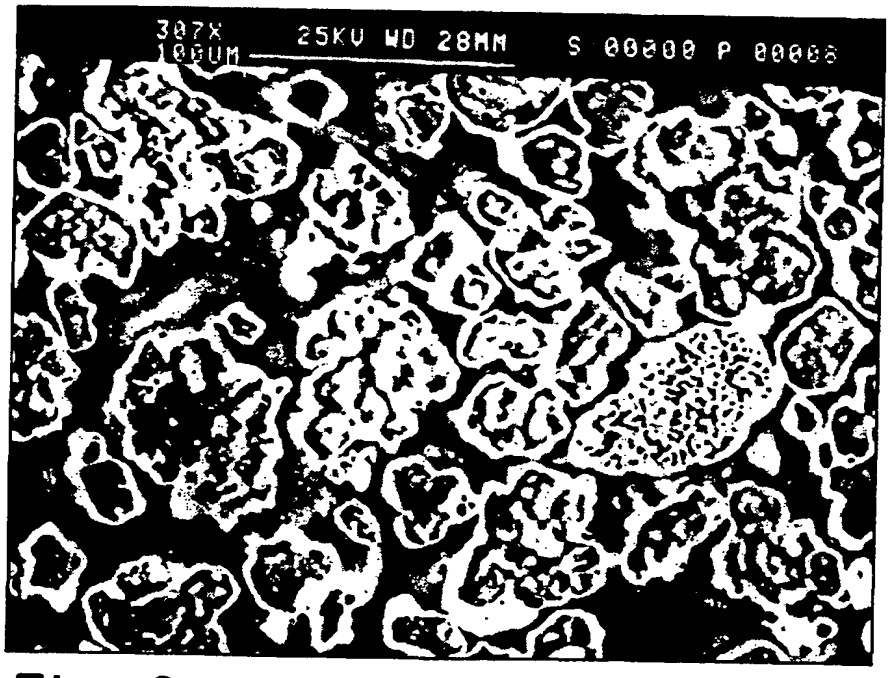

B

Fig. 8 MICROGRAPHS OF METAL COATED ANODES (SHOW IMPROVEMENT OF ENGINEERED METAL COATED CERAMIC MICROSTRUCTURE:-METALLIC PHASE APPEARS LIGHTER)

A). AS-RECEIVED ANODE PLAQUE XXII-1 FROM BATCH 3

B). AS-RECEIVED PLAQUE LXXVIII-8 FROM BATCH 8

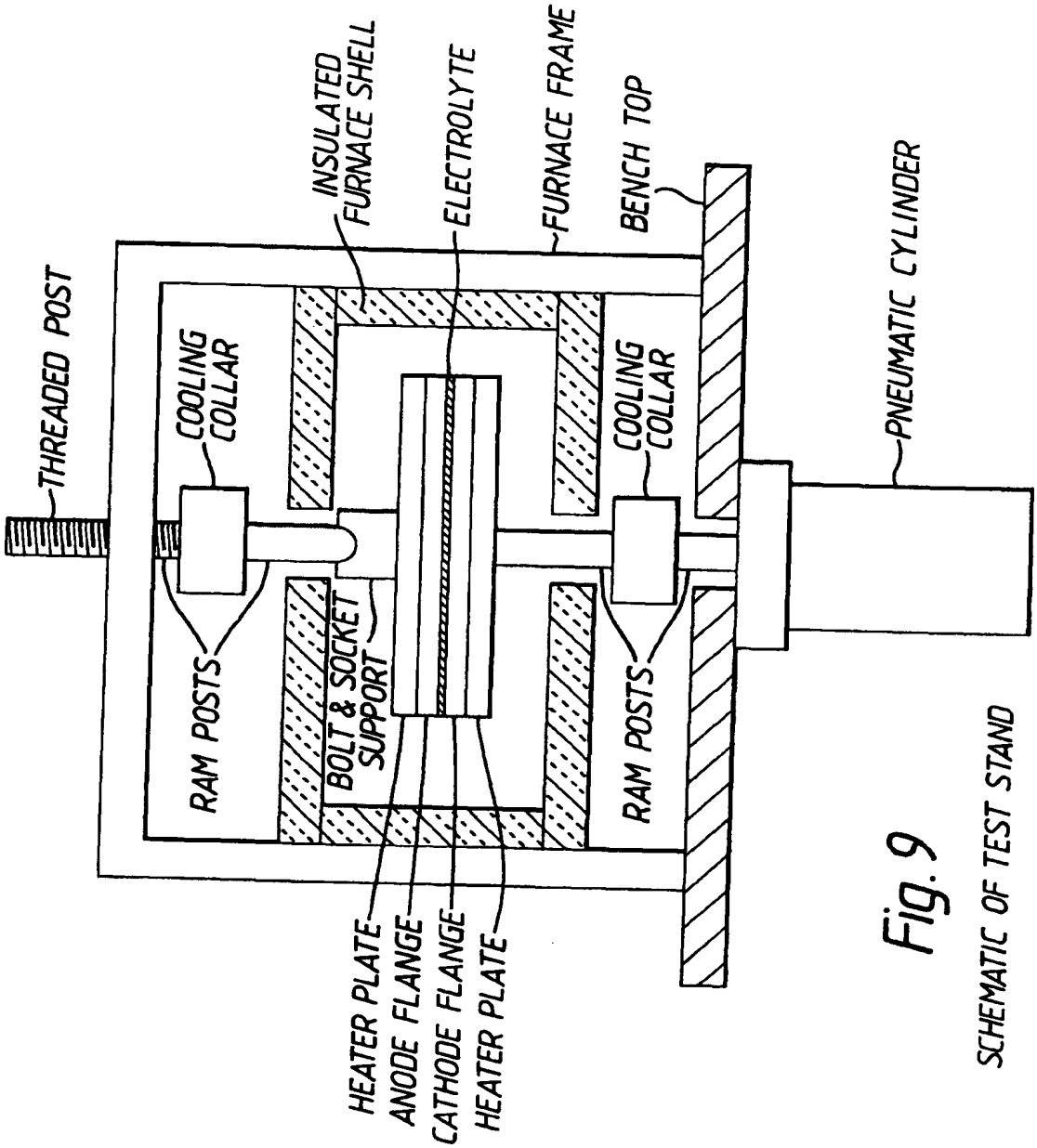

Fig. 9

SCHEMATIC OF TEST STAND

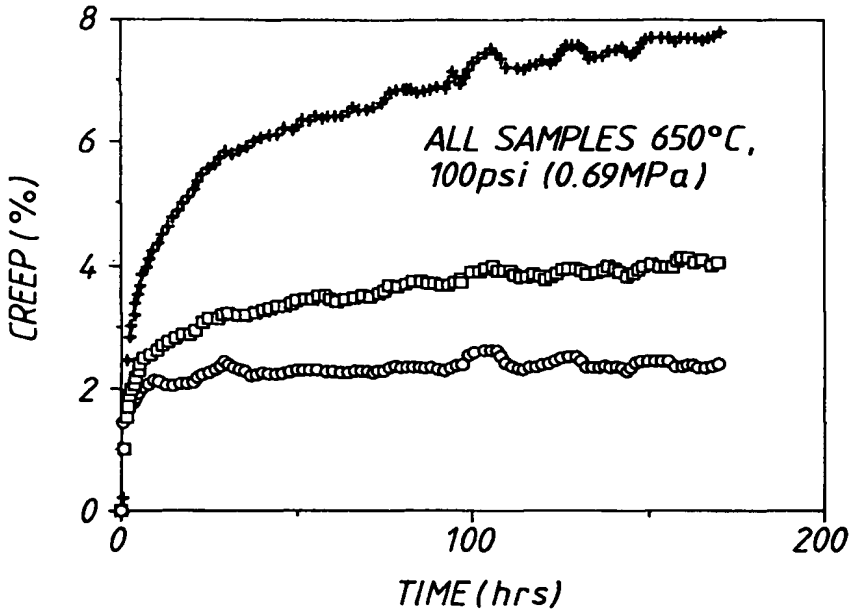

CREEP TEST 2.3.1b-05 (ELECTROLESS PLATED LIFE O_2)

Fig. 10

(19) Europäisches Patentamt
European Patent Office
Office européen des brevets

(11) Publication number : **0 588 536 A3**

(12) **EUROPEAN PATENT APPLICATION**

(21) Application number : **93306951.0**

(51) Int. Cl.[5] : **H01M 4/86**, H01M 8/12

(22) Date of filing : **02.09.93**

(30) Priority : **03.09.92 US 940031**

(43) Date of publication of application :
23.03.94 Bulletin 94/12

(84) Designated Contracting States :
AT BE CH DE DK ES FR GB GR IE IT LI LU MC NL PT SE

(88) Date of deferred publication of search report :
27.04.94 Bulletin 94/17

(71) Applicant : **CERAMATEC INC.**
2425 South 900 West
Salt Lake City, Utah 84119 (US)

(72) Inventor : **Khandkar, Ashok C.**
1921 Nevada Street
Salt Lake City, Utah 84108 (US)

(74) Representative : **Rees, David Christopher et al**
Kilburn & Strode 30 John Street
London WC1N 2DD (GB)

(54) **Creep resistant metal-coated LiFeO2 anodes for molten carbonate and solid oxide fuel cells.**

(57) A porous, creep-resistant, metal-coated, $LiFeO_2$ ceramic electrode for fuel cells. The electrode comprises an ion conducting electrolyte, a layer of unsintered $LiFeO_2$ adjacent the electrolyte and a metal powder in contact with the $LiFe_2$. The metal powder and $LiFeO_2$ are sintered to form a porous electrode.

EP 0 588 536 A3

European Patent Office

EUROPEAN SEARCH REPORT

Application Number
EP 93 30 6951

DOCUMENTS CONSIDERED TO BE RELEVANT

Category	Citation of document with indication, where appropriate, of relevant passages	Relevant to claim	CLASSIFICATION OF THE APPLICATION (Int.Cl.5)
X	EP-A-0 448 517 (INSTITUTE OF GAS TECHNOLOGY) * claims 1,2,9 *	1,3,5,10	H01M4/86 H01M8/12
A	EP-A-0 092 765 (GENERAL ELECTRIC COMPANY) * claims 1,4 *	6	
A	US-A-5 008 163 (JAMES L. SMITH ET AL) * claim 15; example 1 *	1	
A	EP-A-0 111 052 (ENERGY RESEARCH CORPORATION) * page 5, line 1 - line 6; claims 1,5,8 *	1	
A	US-A-3 423 248 (HEINZ-GUNTHER) * column 3, line 11 - line 29 *		

TECHNICAL FIELDS SEARCHED (Int.Cl.5)

H01M

The present search report has been drawn up for all claims

Place of search	Date of completion of the search	Examiner
THE HAGUE	3 March 1994	D'hondt, J

CATEGORY OF CITED DOCUMENTS

X : particularly relevant if taken alone
Y : particularly relevant if combined with another document of the same category
A : technological background
O : non-written disclosure
P : intermediate document

T : theory or principle underlying the invention
E : earlier patent document, but published on, or after the filing date
D : document cited in the application
L : document cited for other reasons

& : member of the same patent family, corresponding document

EPO FORM 1503 03.82 (P0403)